

Friction and Wear Behaviour of Polyester Nanocomposites with Graphene Oxide and Graphite Investigated Through Block-on-ring Test

MARIAN BASTIUREA¹, DUMITRU DIMA², ANTON HADAR³, GABRIEL ANDREI^{1*}

¹Dunarea de Jos University of Galai, Faculty of Engineering, 47 Domneasca Str., 800008, Galati, Romania

²Dunarea de Jos University of Galai, Faculty of Sciences and Environment, 47 Domneasca Str., 800008, Galati, Romania

³Politehnica University of Bucharest, Department of Materials Strength, 060042, Bucharest, Romania

A new class of polyester nanocomposites with graphene oxide and graphite has been obtained through a specific chemical method. Aiming to assess the tribological performance of this type of material, a basic experimental plan has been conceived which includes block-on-ring test, wear rate measurement, Vickers micro hardness test and scanning electron microscopy. Accordingly, the influence of graphene oxide and graphite on coefficient of friction and friction stability were investigated through wear test of nanocomposite blocks against steel rings. At the same time, specific wear rate was inferred in order to examine the mass loss which is strongly dependent on surface micro hardness. After wear test, SEM analysis allowed identification of the transfer film between nanocomposite surface and steel counterpart, and the occurrence of the third body. A careful examination of the friction coefficient recordings has highlighted the effect of the contact condition during the dry sliding test.

Keywords: graphene oxide, graphite, polyester nanocomposite, wear, friction, transfer film

Tribological behavior plays an important role in the performance of all mechanical systems consisting of moving parts. In many applications, as a result of surface tension effects, classical methods of reducing friction with lubricating fluids cannot be used. Therefore, in order to develop reliable mechanisms, the tribological properties of the components must be optimized under dry sliding conditions. Since it was isolated, graphene, a layer of pure carbon atoms just one atom thick has generated a flurry of research activities to identify the mechanical, thermal and tribological properties. Graphene has been obtained in different forms (exfoliated, epitaxial, isolated) and its properties were measured or inferred from related materials, like graphite and carbon nanotubes. Tribological studies using AFM investigated the friction of graphene deposited on different substrate and have found that the friction force decreases monotonically with sample thickness, and converges to that of bulk graphite as the number of layers increases above 5 [1-5]. A rippling-rug effect [1], out-of-plane deformation induced by the AFM tip [2, 3] and cross-linking between graphene neighbor layers [6], are proposed as a possible explanation for this phenomenon. The thickness dependence on friction for graphene is attributed to van der Waals interactions between AFM tip and graphene surface [7], the effect of electron-phonon coupling [8], and the puckering effect [9], which is more dominant with fewer graphene layers [10,11]. The strength of graphene adhesion to the substrate depends on the morphology of the substrate [2,12-14] and contributes to the wear reduction of both film and surface [2]. Frictional properties of epitaxial graphene in ultra-high vacuum is higher than that under similar conditions in ambient conditions. The decrease in the coefficient of friction could be caused by a reduction of the water layer on the sample and on the counter body [12,15-17]. It is reported that increasing the relative humidity, the friction coefficient decreases and this is related to passivation of dangling bonds that form C-O, C-O-C and C-OH [18-20]. Friction can also be affected by different preparation

methods [5, 9, 21-26]. It was found that the friction of graphene under interfacial friction condition has 60° periodicity, and the friction force along armchair orientation is larger than the friction force along zigzag orientation. The observed friction periodicity is due to the lattice rigidity [27-30]. Using Friction Force Microscopy it is showed that graphene oxide exhibit 7-fold enhanced nanoscale friction on their surfaces [31] or more [32], compared to graphene because the graphene oxide possesses abundant hydrophilic groups (hydroxyl and carboxyl groups) that are capable of forming networks of H-bonds [16, 33]. The unusual friction mechanics of graphene oxide is attributed to the intrinsic mechanical anisotropy which is inherently stiff in plane but remarkably flexible out of plane [31], or it contains many surface regions that tend to wear more easily than graphene [14]. The main tribological mechanism of GO additives in water [34, 35], ionic liquid [36], oleic acid [37], esterified bio-oil [38] was observed to be a thin film of GO sheets on the counter ball surface forming a lubricating layer and binding water molecules into contact. The development of a polymer/graphene, graphene oxide or graphite composite coating, improved the friction and wear behavior which were considered to be the result of the formation of uniform transfer film and the spalling of abrasive debris [39-47]. The friction force pattern was used as the fingerprint to reveal the frictional anisotropy on graphite surface [48-52] and weak interplanar van der Waals interactions between planes of graphite are considered to be the origin of its low friction coefficient. Different studies revealed that layer of graphite rolled up and form small roller bearings [51]. It was demonstrated that the interactions between graphite and water or hydrogen vapor greatly influenced its tribological properties [53, 54], and low friction was due to the passivation of dangling bonds by reactive gases [54] or nanocrystallite size [47]. The abrasive wear for graphite is the formation of unstable and incomplete transfer film [53][55]. Albeit, at high loading range, wear debris were unchanged and friction coefficient increased significantly,

* email: gabriel.andrei@ugal.ro

which was explained by transformation of 3D graphite into a 2D turbostratic phase [56]. Graphene used as filler in polymer composite improved frictional and wear behavior of PTFE [57], polyurethane/epoxy [58], phenol formaldehyde [59], UHMWPE [60] due to the formation of chemical bonds between graphene oxide nanosheet and polymer matrix.

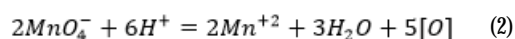
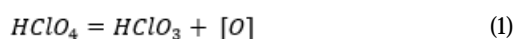
Present work addresses a current challenge concerning the enhancement of mechanical characteristics of polymer nanocomposites based on graphene oxide and graphite. A basic experimental plan has been developed aiming to estimate the friction and wear behavior of polyester nanocomposites. Coefficient of friction test, specific wear rate measurement, Vickers micro hardness and scanning electron microscopy have been considered for investigation of friction stability, transfer film and contact condition effect.

Experimental part

Materials and methods

Graphite (99.6% purity) was purchased from Koh-I-Noor, and the medium size of the graphite particles was of 10.16 μm . Polyester resin (Norsodyne H 13 271 TA) was supplied by Rompolymer. Graphene oxide was synthesized by chemical exfoliation of graphite using a specific method, as described in our previous work [61].

Basic chemical reactions of the method used to obtain graphene oxide nanosheets are given in the following:



Moreover, a graphic representation of the graphite transformation

The polyester composites containing 0.02, 0.04, 0.06, 0.08 and 0.1 wt.% of fillers have been finally prepared. The polyester/graphene oxide composites have been designated as GO 0.02, GO 0.04, GO 0.06, GO 0.08 and GO 0.1, respectively. The polyester/graphite have been designated as G 0.02, G 0.04, G 0.06, G 0.08 and G 0.1, respectively. The pure polyester sample has also been prepared under the same curing condition and have been designated as P.

In order to determine the tribological properties of polyester/graphene oxide and graphite nanocomposites, dry sliding wear tests were carried out on a block-on-ring friction and wear tester (CEMT UMT-2) following ASTM standard G-176 and G-137 in ambient environment. The composite specimens were rotated against a DIN 100Cr6 steel ring. In this study, the wear testing was conducted under three different sliding velocities: 0.25 m/s, 0.5 m/s and 0.75 m/s. In order to keep the same sliding distance, 3000 m, the corresponding wear times were 200 min, 100 min and 66 min, respectively. Tests were conducted at three different loads of 5, 10 and 15 N. All the tests were

performed at room temperature. A number of five repeated tests were conducted for each type of sample. The weight loss was recorded using AB204-S/FACT analytical balance from Mettler Toledo with accuracy of 10^{-4} g and the wear coefficient was subsequently calculated after each testing period. The mass losses were converted to wear volumes using the composite density.

The specific wear rate for each interval could be calculated as follows:

$$W_S = \frac{1}{F_N \vartheta \rho} \cdot \frac{\Delta m}{\Delta t} \quad (1)$$

where:

W_S = specific wear rate, [$\text{mm}^3/\text{N}\cdot\text{m}$], F_N = applied normal force, [N]; ϑ = velocity, [m/s], ρ = density, [kg/mm^3]; Δm = mass loss, [kg], and Δt = time interval, [s].

The Vickers micro hardness of each as-received specimen was measured using a PMT-3 Vickers hardness instrument with a load of 0.2 kg and a dwell time of 10 s. Indentations were made on the surface of each specimen.

The microstructures of the worn surfaces were examined using the scanning electron microscope (SEM) QUANTA 200. The voltage was 15-20 kV, and the surfaces of the samples were previously coated with a thin layer of gold.

Results and discussions

Friction coefficient

Generally, the wear property of composite materials is characterized by the friction coefficient and wear rate. Figures 2(a) and (b) show the friction coefficient behavior vs. sliding distance. However, the running-in stage of polyester/graphene oxide and graphite takes on evidently different tracks. Notably, all the sliding curves for polyester/graphene oxide nanocomposite converge together in the steady stage independent of graphene oxide contents, indicating the same friction coefficient. As shown in figure 2a, the frictional behavior of polyester/graphene oxide is rather unsteady and fluctuates substantially due to less adhesive wear and third-body wear debris accumulation within the sliding contact interface. This indicates that both the friction behaviors of composite during the running-in period and the steady state are changed by the addition of graphene oxide nanoparticles. All of the nanocomposites, GO 0.02, GO 0.04 and GO 0.08 exhibit much longer running-in period (about 1500 m) than pure polyester. The range of the friction coefficient (COF) values for the test performed on all polyester/graphene oxide nanocomposite is between 0.48 and 0.58. The coefficient of friction value for GO 0.02 composite was $\sim 20\%$ lower than that of the pure polyester sample for the steady-state distance. It is clear that the running-in distance is higher in case of polyester/graphene oxide than that in case of polyester, however the coefficient of friction decreases in polyester/graphene oxide than polyester. In fact, during sliding, the friction between the steel ring and specimen surface is less due to the multilayer structure of graphene oxide which provides a lubricating effect of the polyester composite, resulting in a reduced coefficient of friction.

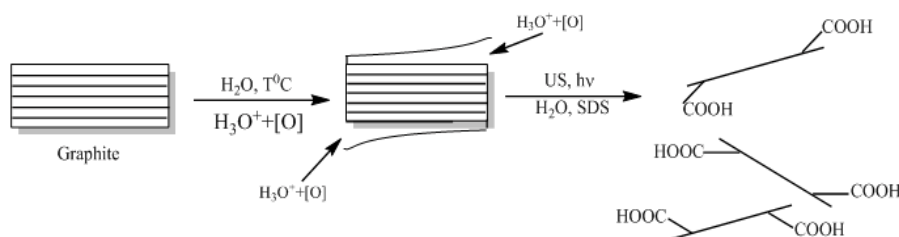


Fig.1. Chemical reactions applied to obtain graphene oxide from graphite [62]

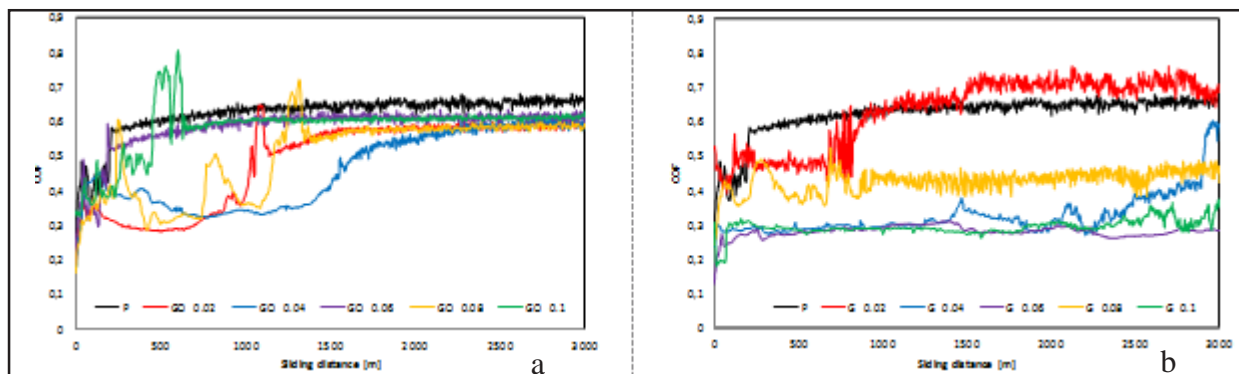


Fig. 2 Friction coefficient of neat polyester and its nanocomposites as a function of sliding distance ($v=0.5$ m/s, $F_N=15$ N)

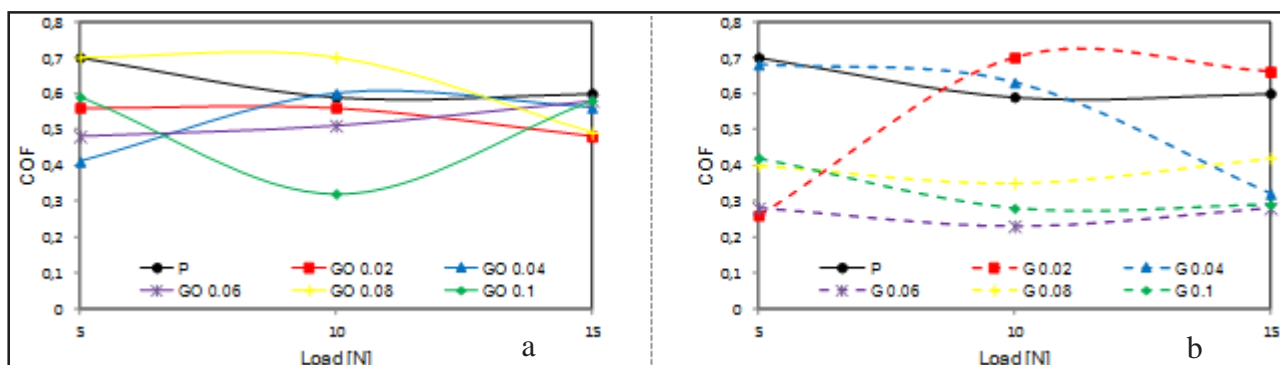


Fig. 3 COF as a function of load ($v=0.5$ m/s) for: a) polyester and polyester/graphene oxide nanocomposite; b) polyester and polyester/graphite nanocomposite

Figure 2b shows the friction coefficient as a function of sliding distance for polyester and polyester/graphite composites. Polyester/graphite exhibit none or a minor irregular running-in behavior. The range of the friction coefficient (COF) values for the test performed on all of the polyester/graphite composite is between 0.28 and 0.66. The lowest results of the friction coefficient, 0.28, was for G 0.06, so that the decrease in COF is 53% compared to pure polyester. The lubricating effect is due to the easy interlayer shearing from graphite structure.

Figure 3 shows the friction coefficients for polyester and polyester/graphene oxide and graphite composite when tested at 0.5 m/s. According to the results, polyester/graphene oxide exhibited lowest friction coefficient when tested at 5 N and 15 N compared to pure polyester. The figure 3 also shows that the lowest COF was obtained for polyester/graphite composite when it was tested at 5 N compared to pure polyester. Surprisingly, the friction coefficients for the GO 0.02 and GO 0.04 composites were lower than those obtained for G 0.02 and G 0.4 composite. It is known that the formation of thin film is attainable whenever there is wear debris at the contact surface between polymeric composite and steel ring. Wear debris form a powdery bed (third body interphase) which is always under *shear flow* during motion of the two surfaces. The nature of the third body is one of the most important factors which determine the overall friction mechanism.

Friction stability

Friction stability was analyzed in terms of percentage ($\mu_m/\mu_{max} \times 100$), where μ_m - means the coefficient of friction and μ_{max} - the maximum value of coefficient of friction in steady-state regime [63]. If friction stability curve is flat, the composite has minimum sensitivity towards load or speed. The stability range of sample was P (84-98%), GO 0.02 (76-96%), GO 0.04 (87-96%), GO 0.06 (78-94%), GO 0.08 (80-96%), GO 0.1 (64-91%), G 0.02 (79-93%), G 0.04

(80-95%), G 0.06 (80-90%), G 0.08 (60-99%), GO 0.1 (65-90%).

The best behavior from these points of view was exhibited by GO 0.04 and the friction stability decreased in following sequence: P, GO 0.1, G 0.04, GO 0.08, G 0.02, GO 0.02, GO 0.06, G 0.06, G 0.1, and GO 0.08. The GO 0.04 range of stability variation (87-96%) was the lowest and the slope was minimal. This was due to the adhesion between graphene oxide and pure polyester which resulted in the thinnest film transfer on ring, as seen in figure 4b-d.

Specific wear rate

The variation of the specific wear rate of the polyester/graphene oxide and graphite nanocomposites with the sliding speed at room temperature is shown in figure 5. When the sliding speed is 0.25 m/s, the maximum decrease in the specific wear rate is about 88% for GO 0.02 and GO 0.06, indicating an efficient ability of nanofiller to improve the wear resistance of polymer matrix at a relatively low sliding speed. For sliding speed of 0.5 m/s the maximum reduction of specific wear rate is around 84-96% for GO 0.06, GO 0.08 and GO 0.1. It can be seen that there may be a general tendency that the specific wear rate from the polyester/graphene oxide composites decreases as the graphene oxide content increases. After that the specific wear rate slightly changes. It is mainly due to the agglomeration of the graphene oxide sheets in the polyester matrix. All polyester/graphite nanocomposites, as can be seen in figure 5b, present a lower specific wear rate than neat polyester. Therefore, there is a decrease in the specific wear rate that is attributed to the presence of the graphite layers in the composite structure.

Addition of graphene oxide and graphite to the polyester matrix obviously reduced the friction coefficient and enhanced wear behavior at ambient temperatures. It indicated that graphene oxide and graphite has acted as a favorable solid lubricant for polyester at ambient temperatures. It can be noticed that both the coefficient of

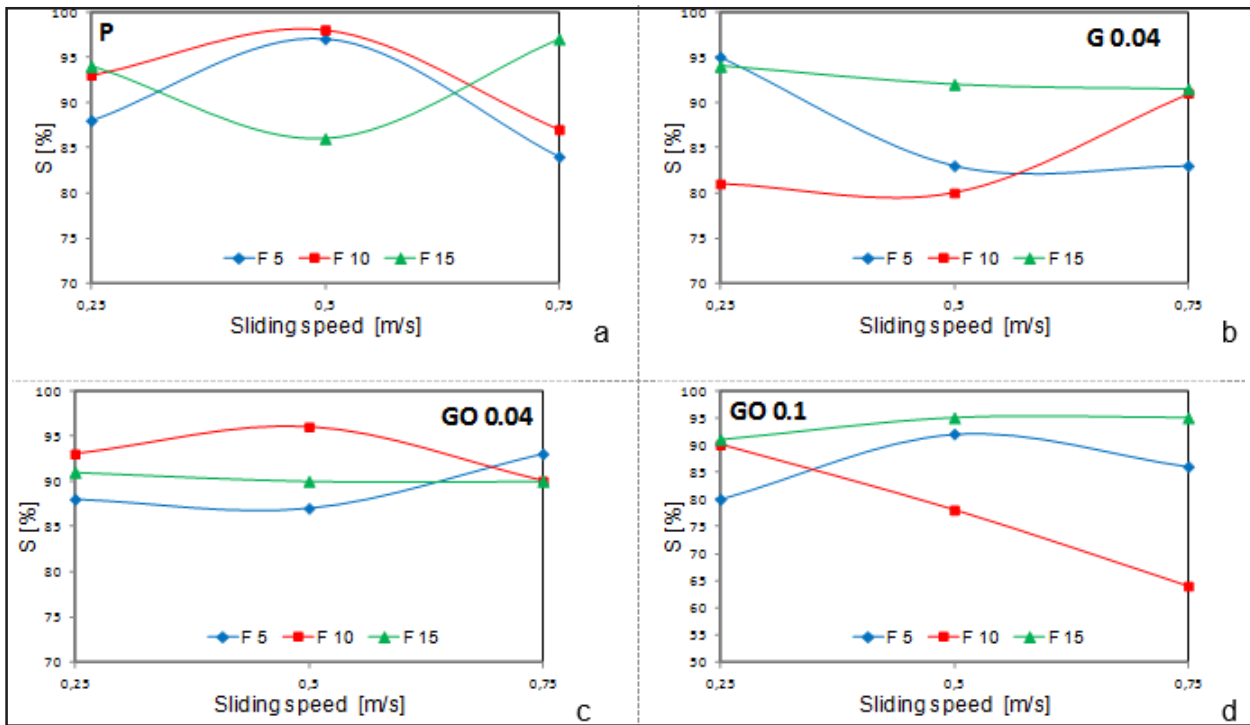


Fig.4 Friction stability as a function of sliding speed for: a) P; b) G 0.04; c) GO 0.04; d) GO 0.01

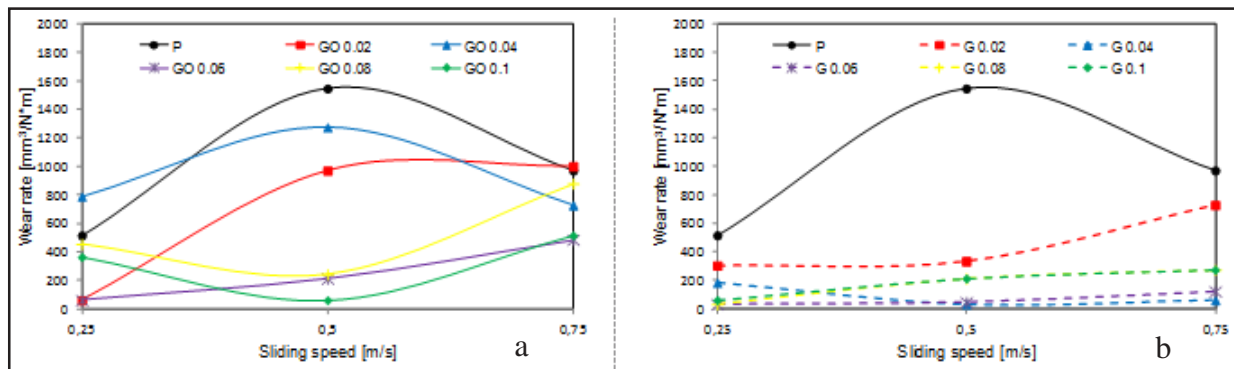


Fig. 5 Specific wear rate as a function of sliding speed (F=10 N): a) polyester and polyester/graphene oxide nanocomposite; b) polyester and polyester/graphite nanocomposite

friction and the specific wear rate show the same tendency with increasing load. The coefficient of friction and the specific wear rate exhibit the same behavior in 35% of test on polyester/graphene oxide and 42% on polyester/graphite composite. The results show clearly that the specific wear rate is correlated to the coefficient of friction.

Vickers micro hardness

Friction and wear behavior of a material during a dry sliding contact against another material is actually influenced by the surface micro hardness. Aiming to highlight the effect of surface micro hardness of polyester nanocomposites on wear characteristics, Vickers micro hardness test were carried out on the surface of the composite specimens.

Figure 6 shows micro hardness values vs. the filler content of graphene oxide and graphite. The hardness of the composite is strongly dependent on the filler content. Vickers micro hardness of the nanocomposites was lower within the range of the graphene oxide and graphite content of our experiments. Vickers micro hardness decreased by 7% up to 58% for GO 0.04 and GO 0.1 nanocomposites compared with the pure polyester, respectively. GO 0.02, GO 0.04 and GO 0.06 has higher Vickers micro hardness than polyester/graphite composite with the same content.

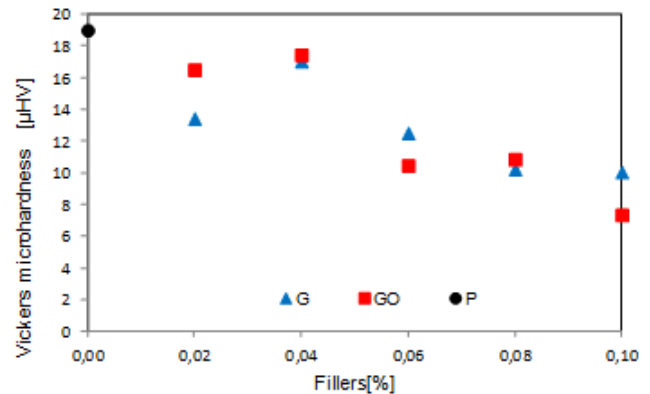


Fig.6. Vickers micro hardness for polyester and its nanocomposites

Taking into account the hardness results, the lower micro hardness surface of polyester/graphene oxide and graphite could exhibit lower wear resistance in sliding contact.

Transfer film and the third body

Generally, when two different materials are subjected to a standard tribological test, wear debris and third body occurrence have to be considered. In particular, when a polymer composite is tested for wear, a transfer film between polymer surface and metal counterpart is expected to occur.

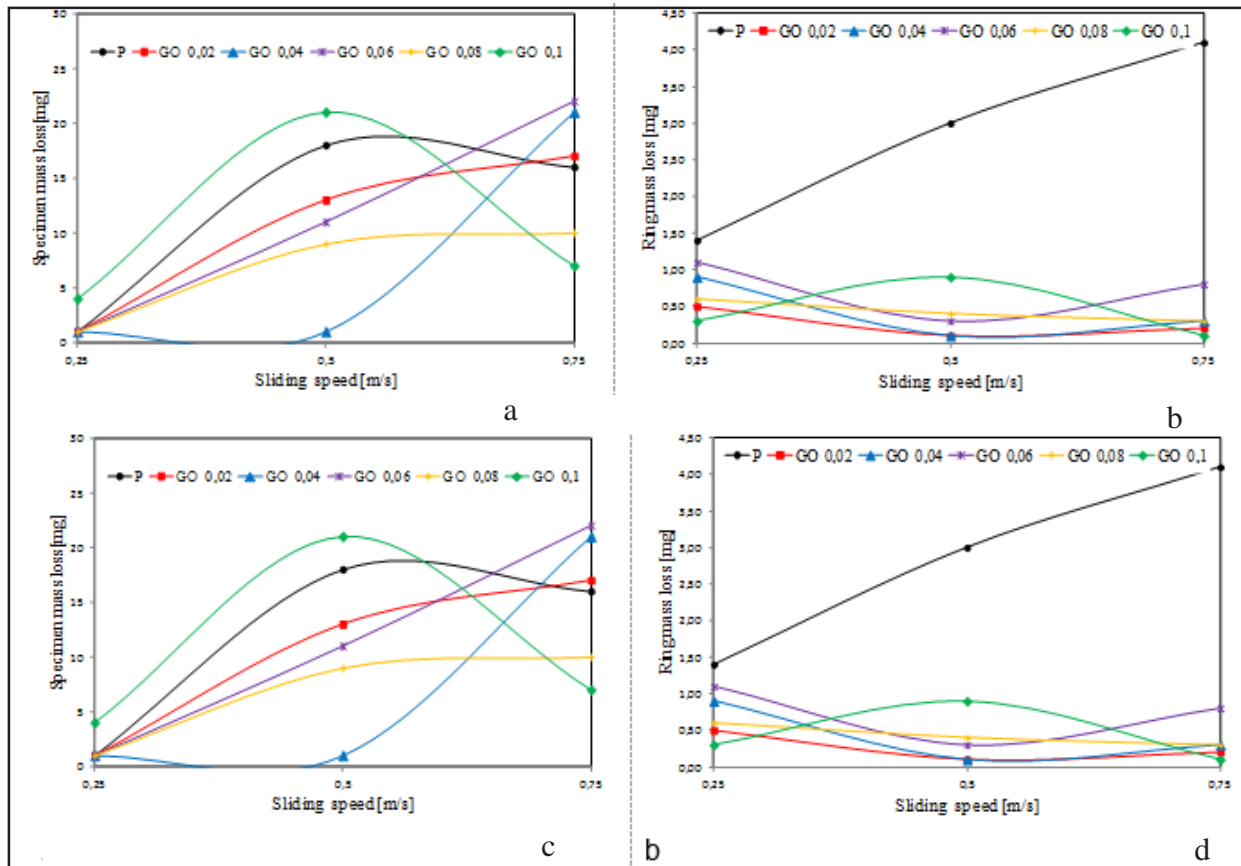


Fig.7. Specimen mass loss and ring mass loss at constant applied load of 5 N: a, b) polyester and polyester/ graphene oxide composite; c,d) polyester and polyester/ graphite composite

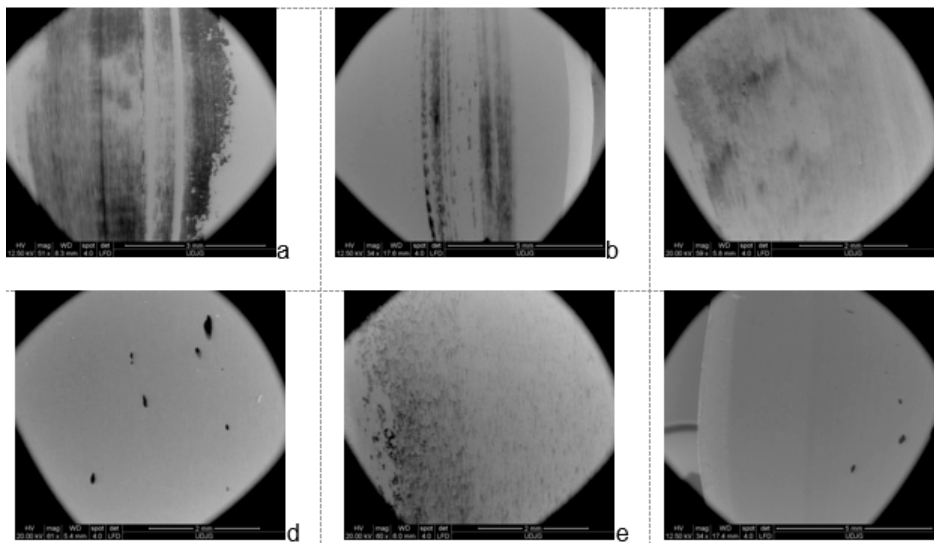


Fig. 8. SEM Images of counterpart ring a) P; b) GO 0.02; c) GO 0.06; d) GO 0.1; e) G 0.02; f) G 0.1 at $v=0.25$ m/s and $F=15$ N

Figure 7 depicts the specimen mass loss and ring mass loss as a function of sliding speed. The aforementioned results confirm that graphene oxide and graphite improve the wear behavior of composite and provide lower abrasive wear of steel ring. Wear depends upon the cohesion of the transfer film, adhesion of the transfer film to the steel ring and the protection of polymer surface against metal asperities provided by the transfer film. The nature of the transferred film on the steel ring surface plays a key role in controlling the wear performance of a polymer composite.

The formation of a thin transfer film on the steel ring is the result of several mechanisms. Most of the wear debris will move towards the nanocomposite specimen surface, but some of them will adhere to the wear surface of the steel ring, and thus they will contribute to the formation of a transfer film. It has been noted that during the steady state of the sliding contact between nanocomposite

specimen and steel ring, the transfer film mainly consists of graphene/graphite fragments embedded in polyester particles. Accordingly, the friction process take place between three material bodies, i.e. nanocomposite surface, steel ring surface and resulting wear particles. It can be noticed that transfer films resulted in case of GO/G nanocomposites are thinner and smaller due to occurrence of spalling and abrasive debris. Also, the transfer film is spread out and discontinuous in case of GO/G nanocomposites with the increase in GO/G content. Previous work has shown that the transfer film could protect the specimens of nanocomposite and the steel ring, decreasing the friction and wear [63]. From figure 8 and figure 9 it can be observed that the wear regime is more abrasive and more adhesive in case of pure polyester/ steel ring contact than that of composite / steel ring contact. Therefore, graphene oxide and graphite are able to replace the thin

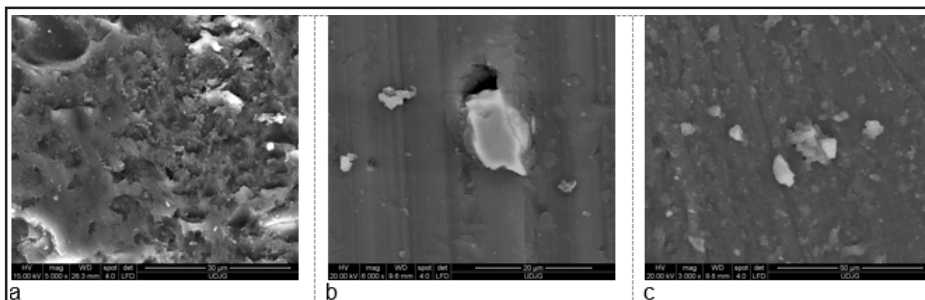


Fig. 9 Worn surface for $v=0.25$ m/s and $F=15$ N of: a)P; b) GO 0.08; c) G 0.08

solid films and reduce adhesion and friction between the two relative sliding parts. The transfer film decrease was accounted for by the combined effect of the third body action (graphene/graphite fragments embedded in polyester particles) and weak interfacial bonding between noncomposite surface and steel ring.

Comparing the wear tracks, the worn surface of nanocomposites seems to be smoother than that of pure polyester (fig. 9). It is clear that the worn surface of the pure polyester was characterized by broadly surface damage and significant tear appeared, with adhesion wear being the major wear form. The adhesive wear mechanism of polyester pull out small pieces of material from surface leading to the formation of cavities. The wear debris form a higher surface transfer film to steel ring, as can see in figure 8. Figure 9a,b shows two abraded surfaces of composites, where some fillers particles embedded in the composite surface may be observed. Cavities development was quasi absent in the case of the polyester nanocomposite. During the sliding contact between the nanocomposite and the steel ring, the presence of graphene oxide / graphite into composite structure lead to the occurrence of abrasion wear mechanism, while in case of the contact between neat polyester and steel ring, the adhesive wear mechanism is prevalent. Graphene oxide and graphite act as a third body, like a roller bearing, avoiding the direct contact of the nanocomposite with the steel ring, and leading to decrease in coefficient of friction.

Conclusions

To sum up, the incorporation of graphene oxide and graphite nanosheets at a very low content into the polyester matrix has led to significantly modified tribological performance. There are several reasons for the advantages given by graphene oxide nanosheets, which include their high specific surface area and enhanced graphene oxide-polyester adhesion. The obtaining of high-performance polyester-GO nanocomposites requires maximal interfacial adhesion between graphene oxide and polyester matrix, as well as an effective load transfer.

Inclusion of graphene oxide and graphite into polyester matrix leads to a better wear behavior of nanocomposites. The results indicate that small amounts of graphene oxide and graphite are able to give reasonably low friction and wear compared to unsteady friction of neat polyester. The significant decrease in friction coefficient in case of polyester/graphene oxide composites compared to neat polyester, was in range of 5-53% when graphene oxide content was 0.02wt.%. In case of polyester/graphite nanocomposite, maximum decrease in coefficient of friction was in range of 19-69% when graphite content was 0.06 wt.%. Graphene oxide was able to reduce friction more than graphite only in case of GO 0.02 in range of 14-55% and for GO 0.04 in range of 1-50% compared to G 0.02 and G 0.04. The specific wear rate was lower in range of 9-84% for GO 0.08 and 67-98% in case of G 0.08. Graphene oxide and graphite have reduced Vickers micro hardness and

transfer film to the steel ring compared to pure polyester, transforming the adhesive wear of pure polyester into abrasive wear. Excellent friction stability was observed during the test of GO 0.04 (87-96%). SEM images shown the occurrence of the third body and the transfer film between nanocomposite and steel ring surface. Further researches have to be performed in order to clarify the wear mechanism which occurs during dry sliding contact between polyester nanocomposites and steel counterparts.

References

1. LEE, C., WEI, X.D., LI, Q.Y., CARPICK, R., et al., Phys. Status Solidi B-Basic Solid State Phys., 246, 2009, 2562-2567.
2. LEE, C., LI, Q., KALB, W., LIU, X.Z., et al., Science (80-), 328, 2010, 76-80.
3. SUN, C., ZHANG, Y., WANG, Y., CHEN, Y., in: Int. Conf. Manip. Manuf. Meas. Nanoscale, 2013, pp. 224-227.
4. GUPTA, S., HEINTZMAN, E., JASINSKI, J., J. Electron. Mater., 43, 2014, 3458-3469.
5. SHIN, Y.J., STROMBERG, R., NAY, R., HUANG, H., et al., Carbon N. Y., 49, 2011, 4070-4073.
6. ZHANG, Q., DIAO, D., BAI, S., HIGUCHI, Y., et al., Tribology Int., 88, 2015, 85-88.
7. LEE, H., LEE, N., SEO, Y., EOM, J., LEE, S., Nanotechnology, 20, 2009, 325701.
8. FILLETER, T., MCCHESENEY, J.L., BOSTWICK, A., ROTENBERG, E., et al., Phys. Rev. Lett., 102, 2009.
9. MARCHETTO, D., HELD, C., HAUSEN, F., WAHLISCH, F., et al., Tribol. Lett., 48, 2012, 77-82.
10. LI, Q., LEE, C., CARPICK, R.W., HONE, J., Phys. Status Solidi Basic Res., 247, 2010, 2909-2914.
11. LEE, C., LI, Q., KALB, W., LIU, X.-Z., et al., Science, 328, 2010, 76-80.
12. CHO, D.-H., WANG, L., KIM, J.-S., LEE, G.-H., et al., Nanoscale, 5, 2013, 3063-9.
13. OU, J., WANG, J., LIU, S., MU, B., et al., Langmuir, 26, 2010, 15830-15836.
14. CHEN, H., FILLETER, T., Nanotechnology, 26, 2015, 135702.
15. MARCHETTO, D., FESER, T., DIENWIEBEL, M., Friction, 3, 2015, 161-169.
16. PENG, Y., WANG, Z., LI, C., Nanotechnology, 25, 2014, 305701.
17. PAOLICELLI, G., TRIPATHI, M., CORRADINI, V., CANDINI, A., VALERI, S., Nanotechnology, 26, 2015, 055703.
18. KUMAR, N., DASH, S., TYAGI, A.K., RAJ, B., Tribol. Int., 44, 2011, 1969-1978.
19. BERMAN, D., ERDEMIR, A., ZINOVEV, A. V., SUMANT, A. V., Diam. Relat. Mater., 54, 2015, 91-96.
20. BHOWMICK, S., BANERJI, A., ALPAS, A.T., Carbon N. Y., 87, 2015, 374-384.
21. KIM, K.S., LEE, H.J., LEE, C., LEE, S.K., et al., ACS Nano, 5, 2011, 5107-5114.
22. CIRCIUMARU, A., ANDREI, G., BIRSAN, I., SEMENESCU, A., Mater. Plast., 46, 2009, 211-214.
23. DELEANU, L., BIRSAN, I.G., ANDREI, G., Mat. Plast., 44, 2007, p. 66.
24. DIMA, D., ANDREI, G., Materwiss. Werksttech., 34, 2003, 349-353.
25. CIUPAGEA, L., ANDREI, G., DIMA, D., MURARESCU, M., Dig. J. Nanomater. Biostructures, 8, 2013, 1611-1619.

26. DIMA, D., MURARESCU, M., ANDREI, G., *Dig. J. Nanomater. Biostructures*, **5**, 2010, 1009-1014.
27. KIM, D.-I., PARK, S.-M., HONG, S.W., JEONG, M.Y., Kim, K.H., *Carbon N. Y.*, **85**, 2015, 328-334.
28. ZHANG, Y., LIU, L., XI, N., WANG, Y., et al., *Sci. China Physics, Mech. Astron.*, **57**, 2014, 663-667.
29. XIAO, J., ZHANG, L., ZHOU, K., LI, J., et al., *Carbon N. Y.*, **65**, 2013, 53-62.
30. KUMAR, N., RADHIKA, R., KOZAKOV, A.T., PANDIAN, R., et al., *Appl. Surf. Sci.*, **324**, 2015, 443-454.
31. KO, J.-H., KWON, S., BYUN, I.-S., CHOI, J.S., et al., *Tribol. Lett.*, **50**, 2013, 137-144.
32. DING, Y.-H., REN, H.-M., CHANG, F.-H., ZHANG, P., JIANG, Y., *Bull. Mater. Sci. Indian Acad. Sci.*, **36**, 2013, 1073-1077.
33. LI, Y., WANG, Q., WANG, T., PAN, G., *J. Mater. Sci.*, **47**, 2011, 730-738.
34. SONG, H.J., LI, N., *Appl. Phys. A Mater. Sci. Process.*, **105**, 2011, 827-832.
35. ELOMAA, O., SINGH, V.K., IYER, A., HAKALA, T.J., KOSKINEN, J., *Diam. Relat. Mater.*, **52**, 2015, 43-48.
36. FAN, X., WANG, L., *J. Colloid Interface Sci.*, **452**, 2015, 98-108.
37. YANG, C., HOU, X., LI, Z., LI, X., et al., *Appl. Surf. Sci.* **2015**
38. XU, Y., PENG, Y., DEARN, K.D., ZHENG, X., et al., *Wear*, **342-343**, 2015, 297-309.
39. WANG, Y., PU, J., XIA, L., DING, J., et al., *Tribol. Lett.*, **53**, 2013, 207-214.
40. LIU, H., LI, Y., WANG, T., WANG, Q., *J. Mater. Sci.*, **47**, 2012, 1867-1874.
41. CHEN, J., LI, J., XIONG, D., HE, Y., et al., *Appl. Surf. Sci.* **2015**.
42. SONG, H.-J., LI, N., YANG, J., MIN, C.-Y., ZHANG, Z., *J. Nanoparticle Res.*, **15**, 2013, 1433.
43. SONG, H.J., LI, N., LI, Y., MIN, C., WANG, Z., *J. Mater. Sci.*, **47**, 2012, 6436-6443.
44. PAN, G., GUO, Q., DING, J., ZHANG, W., WANG, X., *Tribol. Int.*, **43**, 2010, 1318-1325.
45. WU, H., LIU, F., GONG, W., YE, F., et al., *Surf. Coatings Technol.*, **272**, 2015, 25-32.
46. BAI, G., WANG, J., YANG, Z., WANG, H., et al., *Carbon N. Y.*, **84**, 2015, 197-206.
47. CHEN, C., DIAO, D., FAN, X., YANG, L., WANG, C., *Tribol. Lett.*, **55**, 2014, 429-435.
48. LIU, Z., WANG, W., LIU, L., *Appl. Surf. Sci.*, **332**, 2015, 473-479.
49. WILLIAMS, J.A., MORRIS, J.H., Ball, A., *Tribol. Int.*, **30**, 1997, 663-676.
50. SAVAGE, R.H., *J. Appl. Phys.*, **19**, 1948, 1.
51. SPREADBOROUGH, J., *Wear*, **5**, 1962, 18-30.
52. DENG, Z., SMOLYANITSKY, A., LI, Q., FENG, X.-Q., CANNARA, R.J., *Nat. Mater.*, **11**, 2012, 1032-7.
53. ZHU, Z., BAI, S., WU, J., XU, L., et al., *J. Mater. Sci. Technol.*, **31**, 2015, 325-330.
54. LANCASTER, J.K., *Wear*, **34**, 1975, 275-290.
55. ARANGANATHAN, N., BIJWE, J., *Wear*, **330**, 2015, 515-523.
56. KUMAR, N., KOZAKOV, A.T., RAVINDRAN, T.R., DASH, S., Tyagi, A.K., *Tribol. Int.*, **88**, 2015, 280-289.
57. BHARGAVA, S., KORATKAR, N., BLANCHET, T.A., *Tribol. Lett.*, **59**, 2015, 17.
58. XIA, S., LIU, Y., PEI, F., ZHANG, L., et al., *Polymer (Guildf.)*, **64**, 2015, 62-68.
59. YANG, M., ZHANG, Z., ZHU, X., MEN, X., REN, G., *Friction*, **3**, 2015, 72-81.
60. TAI, Z., CHEN, Y., AN, Y., YAN, X., XUE, Q., *Tribol. Lett.*, **46**, 2012, 55-63.
61. BASTIUREA, M., RODEANU, M.S., DIMA, D., MURARESCU, M., ANDREI, G., *Dig. J. Nanomater. Biostructures*, **10**, 2015, 521-533.
62. BASTIUREA, M., DIMA, D., ANDREI, G., *Mat. Plast.*, **55**, no. 1, 2018, p. 102
63. KOLLURI, D., GHOSH, A.K., BIJWE, J., *Wear*, **266**, 2009, 266-274.

Manuscript received: 9.01.2018